Adsorption 6, 53–59 (2000)

Sorption and Diffusion of *p*-Xylene and *o*-Xylene in Aluminophosphate Molecular Sieve $AlPO_4$-11

CÉLIO L. CAVALCANTE, JR., DIANA C.S. AZEVÊDO, IRLA G. SOUZA AND A. CRISTINA M. SILVA
Universidade Federal do Ceará, Departamento de Engenharia Química GPSA, Grupo de Pesquisas em Separações por Adsorção, Campus do Pici, Bl. 710 - Fortaleza-CE, 60.455-760, Brazil
celio@deq.ufc.br

ODELSIA L.S. ALSINA AND VERÔNICA E. LIMA
Universidade Federal da Paraíba, Departamento de Engenharia Química Campina Grande, PB, 58109-970, Brazil

ANTONIO S. ARAUJO
Universidade Federal do Rio Grande do Norte, Departamento de Química Natal, RN, 59078-970, Brazil

Received October 21, 1998; Revised June 25, 1999; Accepted September 2, 1999

Abstract. This paper presents experimental results for equilibrium and diffusion of C_8 aromatics in laboratory synthesised crystals of $AlPO_4$-11. The samples were prepared by the hydrothermal method, starting from pseudobohemite (CONDEA), 85% phosphoric acid, water and di-isopropilamine as organic template. Adsorption and diffusion data were obtained mainly by gravimetry at temperatures between 60–100°C. Saturation capacities were found in the range of 4 wt%. Equilibrium constants were estimated using virial plots yielding heats of adsorption between 10–12 Kcal/mol at low coverage. Intracrystalline diffusivities at higher temperatures (150–180°C) were also measured, using the Zero-Length-Column (ZLC) method. Diffusivities from both methods (gravimetric and ZLC) agreed reasonably well and followed a typical Arrhenius behaviour, with low activation energy (ca. 7 Kcal/mol).

Keywords: equilibrium, diffusion and kinetics, $AlPO_4$-11 molecular sieve

Introduction

The aluminophosphate molecular sieves ($AlPO_4$-*n*), first reported by Wilson et al. (1982), represent the first class of oxide materials free of silica. Most of these materials exhibit properties similar to those of zeolites, indicating that they can be used as adsorbents, catalysts or catalyst supports in several chemical processes (Rabo et al., 1989; Davis, 1991; Sierra et al., 1994). The main advantages of the aluminophosphate molecular sieves, as compared to other supports, are related to the possibility of varying the following physicochemical properties: pore size, pore shape, dimensions of the pore system, presence or absence of cages, acid sites properties, surface properties, void volume and framework compositions (Araujo et al., 1997).

Microporous crystalline $AlPO_4$-11 has an AEL topology and is a member of the aluminophosphate molecular sieves family, which exhibits unidimensional 10-membered ring channels. The pore opening is elliptical with about 3.9×6.3 Å. The symmetry of $AlPO_4$-11 is orthorhombic with the following unit cell dimensions: $a = 13.5336$ Å, $b = 8.4821$ Å and $c = 8.3703$ Å (Treacy et al., 1996).

C_8 aromatics are the starting material for the production of dimethylteraphtalate (DMT), teraphtalic acid (TPA), poliethylene teraphtalate (PTA), largely used in the modern plastics industry. C_8 aromatics separation processes using selective adsorption on aluminosilicate molecular sieves, mainly zeolites X or Y, are currently among the most important industrial large-scale processes (e.g. Sorbex^{TM}). There have been attempts to synthesise aluminophosphate molecular sieves to replace zeolites as adsorbents for xylenes separations. For instance, $AlPO_4$-5 and $AlPO_4$-11 have been reported as ortho-selective (Barthomeuf and Mallmann, 1990; Chiang et al., 1991).

In this paper, we report experimental data for equilibrium and diffusion of *p*-xylene and *o*-xylene in crystals of $AlPO_4$-11, at temperatures between 60–180°C. Equilibrium data are correlated using Langmuir, virial and Dubinin plots, in order to estimate equilibrium constants, saturation capacities and heats of adsorption at low coverage. Intracrystalline diffusivities are reported from two different experimental methods (gravimetric and ZLC) with reasonable agreement among them.

Experimental

Synthesis and Characterisation

The $AlPO_4$-11 crystals were synthesised by the hydrothermal method, starting from pseudobohemite (CONDEA), 85% orthophosphoric acid (MERCK), water and di-isopropilamine (RIEDEL) as organic template. The reactants were mixed in the following stoichiometric molar composition:

$$1.0\ \text{iso-}(C_3H_7)_2\,NH : 1.0Al_2O_3 : 1.0P_2O_5 : 80H_2O$$

The synthesis procedure involved the following steps: (i) pseudobohemite was slurred in half of total volume of water; (ii) orthophosphoric acid was diluted to the rest of water and; (iii) the orthophosphoric acid solution was added to the aluminium hydroxide slurry. The mixture thus obtained was aged for two hours at room temperature under continuous stirring until pH stabilisation. At last di-isopropilamine was added to the mixture to form a reactive hydrogel, which was charged into a PTFE vessel and autoclaved at 170°C for three days, under autogenic pressure. The resulting material was then washed with deionized water and dried at 100°C for one day. Finally, the sample was calcined at 500°C under 60 mL·min^{-1} oxygen flow, until complete removal of the organic template.

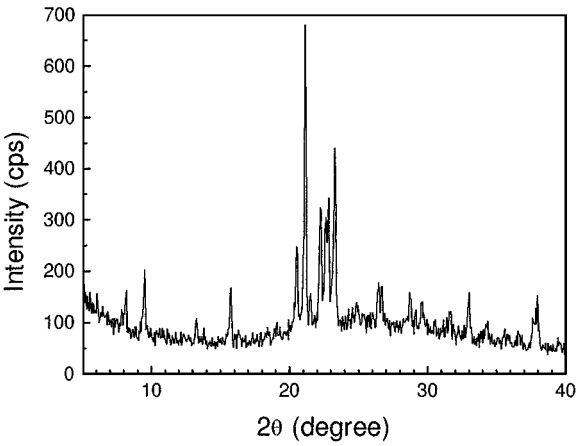

Figure 1. XRD pattern of the $AlPO_4$-11 sample.

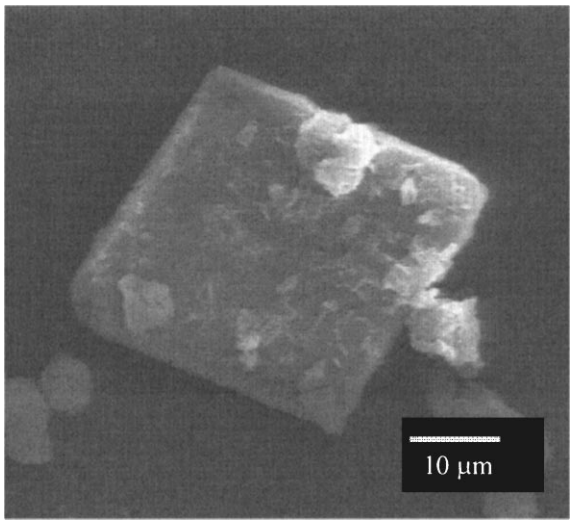

Figure 2. Scanning electron micrograph of the $AlPO_4$-11 crystal.

A full detailed characterisation of these samples has been reported by Araujo et al. (1999). X-ray diffraction pattern of the sample was recorded on a Rigaku diffractometer using Cu-K_α radiation, and the diffraction angle ranging from 5 to 40° (Fig. 1). The morphology and size of the crystals were determined by scanning electron microscopy, in a Zeiss DSM microscope, at 10 Kv and 77 μA (Fig. 2). Adsorption isotherms of nitrogen on the aluminophosphate crystals were measured with an Accusorb 2100E (Micrometrics) at room temperature. Table 1 summarises the main characteristics of the sample.

Table 1. Characteristics of $AlPO_4$-11 sample.

Crystal size	43 μm
Pore volume	14 cm^3/g
Surface area	104.8 m^2/g
Main diffusional channel	3.9 × 6.3 Å (10-Ring elliptical)

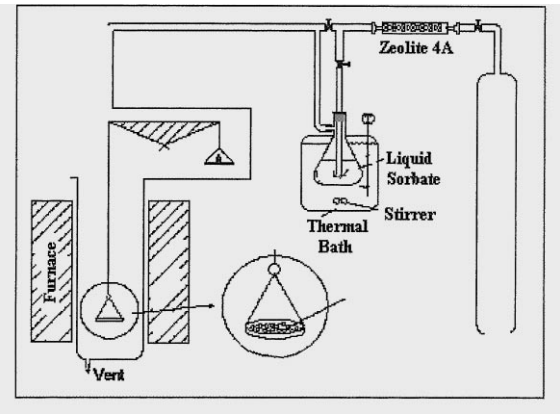

Figure 3. Gravimetric experimental set-up.

Equilibrium and Diffusion Measurements

For equilibrium measurements a CAHN electrobalance Model 2000, precision 1 μg, was used, as schematically shown in Fig. 3. The zeolite sample (≈15 mg) was previously regenerated inside the microbalance oven by slowly heating under dry nitrogen flow up to temperatures of 350°C. Sorbate fluid phase concentrations were established by setting the thermal bath temperature corresponding to a desired vapour pressure of the pure component. Isotherm data points were collected following the weight increase at the balance up to equilibrium at each fluid phase concentration. Low concentration diffusion coefficients estimates could be carried out by following the weight increase with time for the first isotherm run at each temperature.

Diffusion estimates were also made using the Zero-Length Column (ZLC) method, at temperatures of 150 and 180°C. A sketch of the experimental set-up is shown in Fig. 4. The sorbent (≈2 mg) was set in a monolayer between sintered disks inside an oven and previously regenerated at 300°C for at least 12 hours before each experiment. The sample was then taken up to complete saturation with the sorbate at a given concentration (established through the thermal bath temperature) and, at time zero, submitted to a purge with an inert gas at the same flow rate. The variation of concentration with time is then followed in a Flame Ionisation Detector and matched to a Fickian diffusion model to allow estimates for the intracrystalline diffusivities.

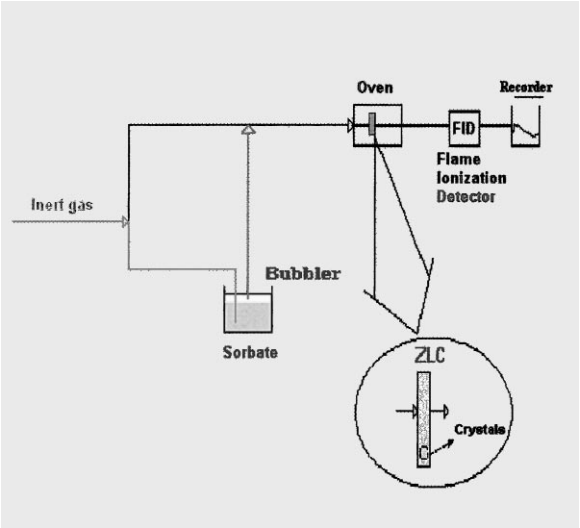

Figure 4. ZLC experimental set-up.

Results and Discussion

Equilibrium

Equilibrium isotherms at temperatures of 60, 80 and 100°C are shown in Figs. 5 and 6. Full lines are Langmuir fits of the experimental data. Table 2 shows the estimated Langmuir parameters from the fit of the experimental data. Saturation capacities up to 4 wt% are

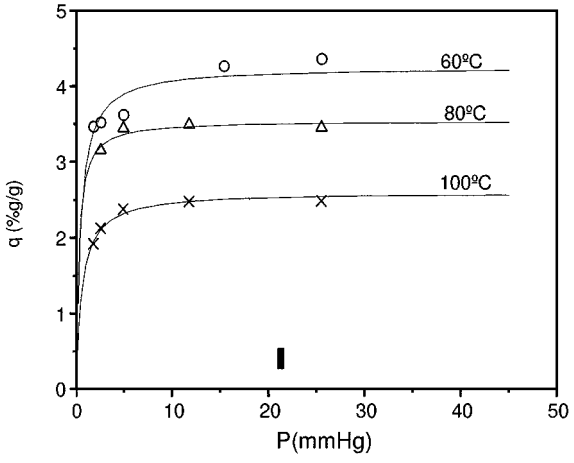

Figure 5. Equilibrium data of *o*-xylene in $AlPO_4$-11. Straight lines are Langmuir fits of the data.

Table 2. Parameters from equilibrium data of xylenes in $AlPO_4$-11.

		Langmuir model			Dubinin model	Virial model
	Temp. (°C)	b (mm Hg^{-1})	q_s (%g/g)	K (dimensionless)	q_s (%g/g)	K (dimensionless)
o-Xylene	60	2.205	4.250	31,200	4.349	68,900
	80	3.662	3.543	45,800	3.566	37,900
	100	1.653	2.597	16,000	2.558	10,100
p-Xylene	60	1.946	3.791	24,600	3.819	137,000
	80	2.202	2.783	21,600	3.052	53,700
	100	2.887	2.488	26,800	2.487	26,300

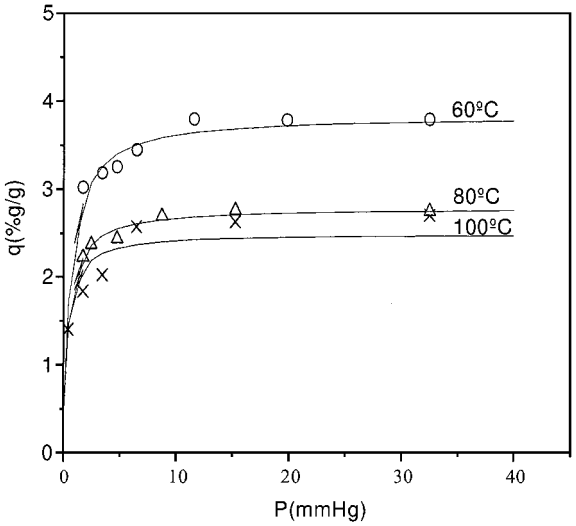

Figure 6. Equilibrium data of *p*-xylene in $AlPO_4$-11. Straight lines are Langmuir fits of the data.

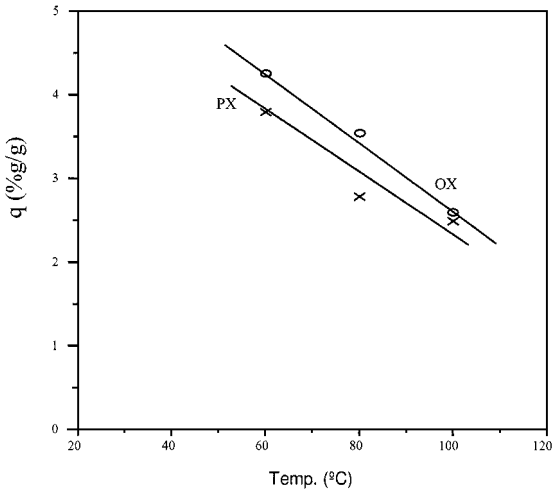

Figure 7. Temperature dependence of saturation capacities of *p*-xylene and *o*-xylene in $AlPO_4$-11.

observed, much lower than what was observed (about 10 wt%) for the same sorbates in $AlPO_4$-5 (Chiang et al., 1991). Figure 7 shows the usual decrease of saturation capacities with temperature, similar to free liquid behaviour, as previously observed for alkanes in silicalite (Cavalcante Jr. and Ruthven, 1995).

Experimental data, plotted according to the virial isotherm (Eq. (1)), are shown in Fig. 8 for *p*-xylene.

$$\ln\left(\frac{P}{q}\right) = \ln\left(\frac{1}{K}\right) + 2A_1 q + \frac{3}{2}A_2 q^2 + \cdots \quad (1)$$

$$K = K_0 \exp\left(\frac{-\Delta U_0}{RT}\right) \quad (2)$$

$$-\Delta H_0 = -\Delta U_0 + RT \quad (3)$$

Equilibrium constants at low coverage estimated from the virial plots are shown in Table 2 and Fig. 9,

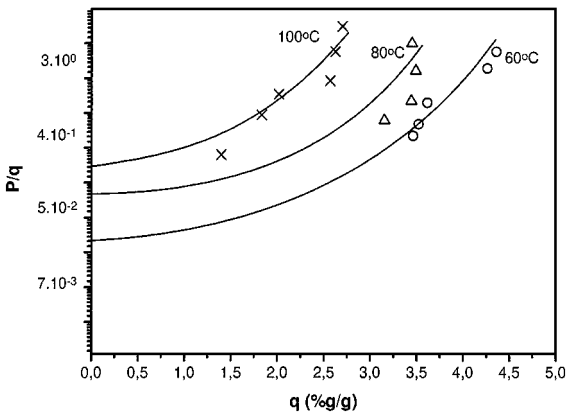

Figure 8. Virial plots of *p*-xylene equilibrium data in $AlPO_4$-11. Full lines extrapolation to $q = 0$ yield estimate of equilibrium constant K, Eq. (1).

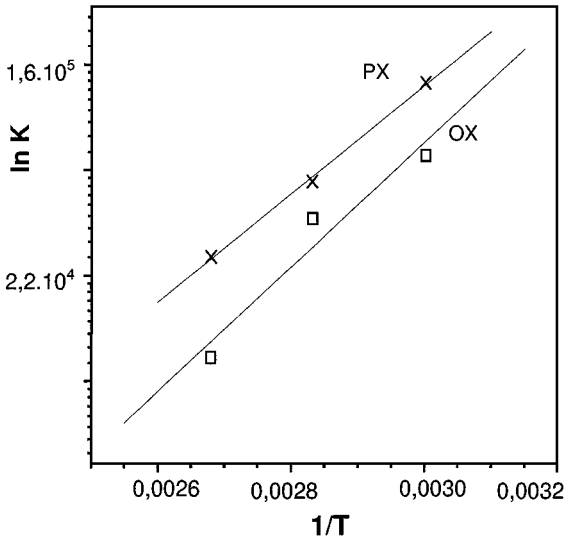

Figure 9. vant Hoff plots for *o*- and *p*-xylene in $AlPO_4$-11, Eq. (2).

yielding estimates of adsorption heat at low coverage (Eqs. (2) and (3)) of 10.2 Kcal/mol for *o*-xylene and 11.7 Kcal/mol for *p*-xylene, slightly lower than the values for the same sorbates in $AlPO_4$-5 (Chiang et al., 1991).

Applying Dubinin's model (Eqs. (4)–(7)), the equilibrium data may be plotted as shown in Fig. 10. Saturation capacities obtained from extrapolation of the data in Fig. 10 to zero potential are also listed in Table 2, showing agreement with the values that were predicted

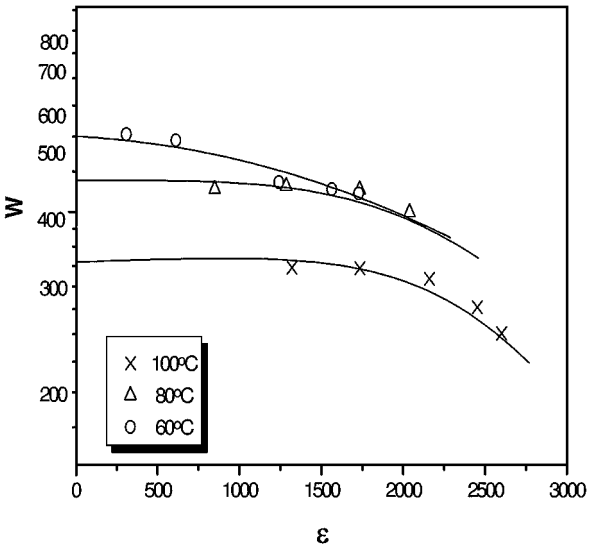

Figure 10. Dubinin plot for *o*-xylene in $AlPO_4$-11, Eq. (4).

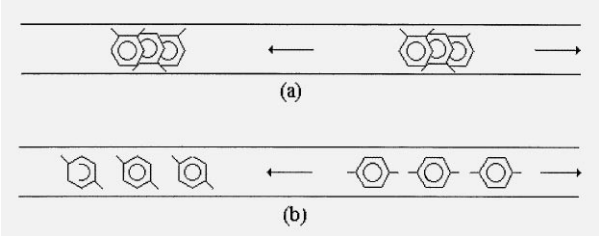

Figure 11. Packing configurations of xylenes in channels of $AlPO_4$-*n*. (a) *o*-xylene; (b) *p*-xylene (Chiang et al., 1991).

from the Langmuir fitting.

$$W = W_0 \exp(-k\varepsilon^2) \tag{4}$$

$$\varepsilon = -RT \ln\left(\frac{P}{P_s}\right) \tag{5}$$

$$W = q V_m \tag{6}$$

$$W_0 = q_s V_m \tag{7}$$

The equilibrium data indicate that, at low coverage, *p*-xylene is preferentially adsorbed as compared to *o*-xylene (*K* values for *p*-xylene are higher than those for *o*-xylene). On the other hand, *o*-xylene shows higher saturation capacities for the pure component as compared to *p*-xylene. This system thus shows an interesting behaviour of some para-selectivity at low coverages and some ortho-selectivity at higher coverages. This was also observed for $AlPO_4$-5 (Chiang et al., 1991). They have nicely demonstrated that *o*-xylene molecule can pack much more closely in the channel (face-to-face), as compared to *p*-xylene (see Fig. 11). This seems to happen also with $AlPO_4$-11, according to our data.

Diffusion

Low concentration intracrystalline diffusion coefficient values were estimated using both gravimetric and ZLC methods. The experimental data were correlated using a simple isothermal Fickian transport diffusion model in one direction (Eq. (8)), with the appropriate boundary conditions for each experimental scheme (Kärger and Ruthven, 1992).

$$\frac{\partial q}{\partial t} = D\left(\frac{\partial^2 q}{\partial x^2}\right) \tag{8}$$

Illustration of experimental data and model estimate for gravimetric runs (60–100°C) are shown in Fig. 12,

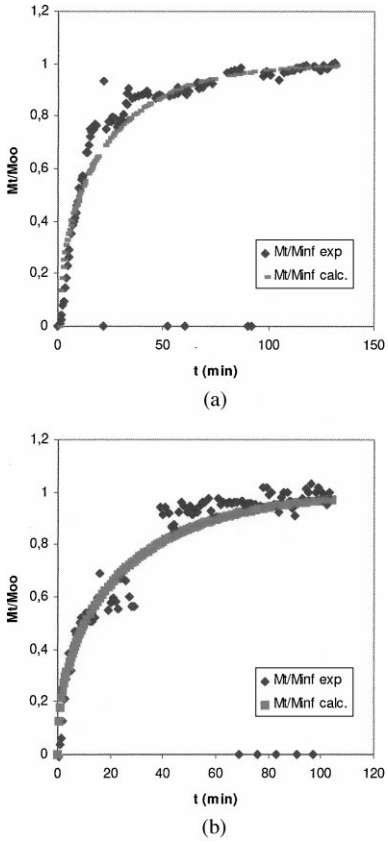

Figure 12. Gravimetric diffusion data for $AlPO_4$-11. (a) *o*-xylene and; (b) *p*-xylene at 80°C.

with reasonable agreement of experimental data and model.

ZLC runs were also performed at higher temperatures (150–180°C). The curve shown in Fig. 13 illustrates the method and shows a good agreement of the data to the model.

A summary of the experimental diffusion coefficient estimates are shown in Table 3 and an Arrhenius plot is

Table 3. Intracrystalline low concentration diffusivities estimates for xylenes in $AlPO_4$-11.

	Temp. (°C)	D (cm^2/s)	Method
o-Xylene	60	7.5×10^{-12}	Gravimetric
	100	1.7×10^{-11}	Gravimetric
	150	3.3×10^{-11}	ZLC
	180	1.4×10^{-11}	ZLC
p-Xylene	60	1.5×10^{-11}	Gravimetric
	80	6.5×10^{-11}	Gravimetric
	150	9.0×10^{-11}	ZLC

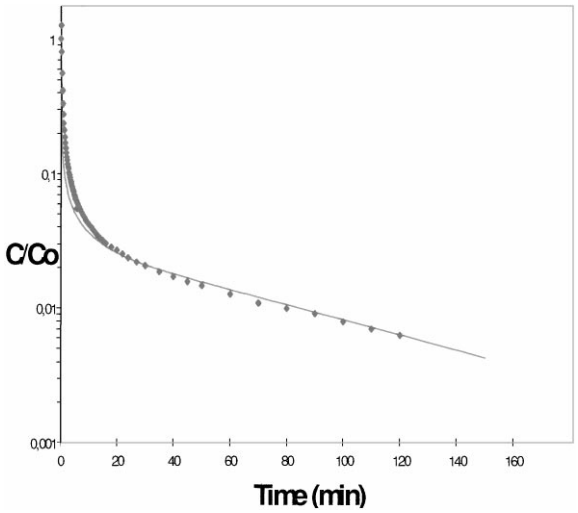

Figure 13. ZLC experimental results for *p*-xylene at 150°C. Full line represents Fickian model theoretical curve.

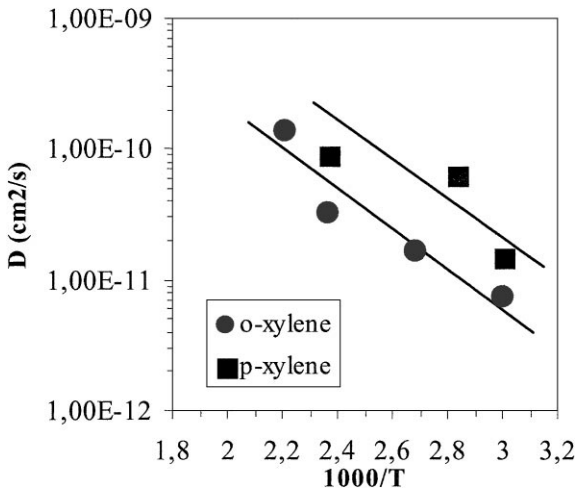

Figure 14. Arrhenius plot of diffusivities of *o*-xylene and *p*-xylene in $AlPO_4$-11.

shown on Fig. 14. Diffusivity values for *p*-xylene are about 3–4 times higher than the values for *o*-xylene. It may be also observed that diffusivity values are about 2 orders of magnitude lower than those for silicalite (for both *p*- and *o*-xylene) at the same conditions (Kärger and Ruthven, 1992). Activation energies were estimated as ≈7 Kcal/mol for both xylene isomers in $AlPO_4$-11. For silicalite, Kärger and Ruthven (1992) report activation energies of the same order of magnitude.

Conclusions

The hydrothermal synthesis process of aluminophosphate molecular sieve $AlPO_4$-11 produced good crystals with typical orthorombic morphology. Both X-ray diffraction and SEM-scanning electron microscope have been used for the characterization of the sample. A thorough survey of equilibrium and diffusion of *p*-xylene and *o*-xylene in $AlPO_4$-11 crystals was performed, for temperatures between 60 and 180°C. Our results indicate that, at low concentrations in the adsorbed phase, both diffusion and equilibrium favours *p*-xylene. However, at saturation capacities, equilibrium favours *o*-xylene, probably due to face-to-face packing orientation. Capacities limited to ≈4 wt% may hinder potential applications of this material to separate xylene isomers, since commercial processes currently employed for *p*-xylene separation use zeolites with capacities as high as 12–15 wt%.

Nomenclature

$A_1, A_2 \ldots$	Virial coefficients
D	Intracrystalline diffusivity
$-\Delta H_0$	Heat of adsorption at low coverage
K	Equilibrium constant
k	Constant in Eq. (4)
P	Pressure
P_s	Saturation pressure
q	Adsorbed phase concentration
q_s	Saturation capacity
R	Gas constant
t	Time
T	Temperature
V_m	Molar volume
$-\Delta U_0$	Internal energy at low coverage
W	Adsorbed volume
W_0	Adsorbed volume at saturation
x	Co-ordinate
ε	Adsorption potential, Eq. (5)

Acknowledgments

The authors gratefully acknowledge financial support from CNPq (Conselho Nacional de Desenvolvimento Científico e Tecnológico), PET/CAPES (Programa Especial de Treinamento-CAPES) and Copene Petroquímica do Nordeste S/A.

References

Araujo, A.S., J.C. Diniz, A.O.S. Silva, and R.A.A. Melo, "Hydrothermal Synthesis of Cerium Aluminophosphate," *J. Alloys and Comp*., **250**, 532–537 (1997).

Araujo, A.S., V.J. Fernandes, Jr., A.O.S. Silva, and J.C. Diniz, "Evaluation of the ALPO-11 Crystallinity by Thermogravimetry," *J. Therm. Anal. and Calorim*., **56**, 151–157 (1999).

Barthomeuf, D. and A. Mallmann, "Adsorption of Aromatics in NaY and $AlPO_4$-5. Correlation with the Sorbent Properties in Separations," *Ind. Eng. Chem. Res*., **29**, 1435–1438 (1990).

Cavalcante, C.L., Jr. and D.M. Ruthven, "Adsorption of Branched and Cyclic Paraffins in Silicalite. I. Equilibrium," *Ind. Eng. Chem. Res*., **34**, 177–184 (1995).

Chiang, A.S.T., C.K. Lee, and Z.H. Chang, "Adsorption and Diffusion of Aromatics in $AlPO_4$-5," *Zeolites*, **11**, 380–386 (1991).

Davis, M.E., "Zeolites and Molecular Sieves: Not Just Ordinary Catalysts," *Ind. Eng. Chem. Res*., **30**, 1675–1683 (1991).

Kärger, J. and D.M. Ruthven, *Diffusion in Zeolites and Other Microporous Solids*, Wiley, New York, 1992.

Rabo, J.A., R.J. Pellet, P.K. Coughlin, and E.S. Shamshoum, *Zeolites as Catalysts, Sorbents and Builders: Applications and Innovations*, H.E. Karge and J. Weitkamp (Eds.), Elsevier, Amsterdam, 1989.

Sierra, L., J. Patarin, C. Deroche, H. Gies, and J.L. Guth, "Novel Molecular Sieves of the Aluminophosphate Family: $AlPO_4$ and Substituted Derivatives with the LTA, FAU and AFR Structure-Types," *Zeolites and Related Microporous Materials: State of The Art 1994*, J. Weitkamp, H.G. Karge, H.P. Feifer, and W. Hölderich (Eds.), pp. 2237–2244, Elsevier, 1994. Studies in Surface Science and Catalysis, 84.

Treacy, M.M.J., J.B. Higgins, and R. von Ballmoos, *Collection of Simulated XRD Powder Patterns for Zeolites*, 3rd edn. Elsevier, New York, 1996.

Wilson, S.T., B.M. Lok, C.A. Messina, T.T. Cannan, and E.M. Flanigen, "Aluminophosphate Molecular Sieves: A New Class of Microporous Crystalline Inorganic Solids,". *J. Am. Chem. Soc.*, **104**, 1146–1150 (1982).